Applied Catalysis A: General 355 (2009) 123–131

Contents lists available at ScienceDirect

Applied Catalysis A: General

journal homepage: www.elsevier.com/locate/apcata

Silica supported tungsta-zirconia catalysts for hydroisomerization–cracking of long alkanes

Mariana Busto [a], María E. Lovato [a], Carlos R. Vera [a], Kiyoyuki Shimizu [b], Javier M. Grau [a,*]

[a] Instituto de Investigaciones en Catálisis y Petroquímica – INCAPE – (FIQ-UNL, CONICET), Santiago del Estero 2654, 3000 Santa Fe, Argentina
[b] Council for Science and Technology Policy, Cabinet Office (AIST-MITI), 3-1-1 Kasumigaseki, Chiyoda-ku, Tokyo 100-8970, Japan

ARTICLE INFO

Article history:
Received 2 May 2008
Received in revised form 1 December 2008
Accepted 5 December 2008
Available online 11 December 2008

Keywords:
Supported zirconia
Silica
Tungsten-zirconia
Hydroisomerization
Hydrocracking
Long alkanes

ABSTRACT

New acidic materials with fairly uniform mesoporous texture were synthesized by deposition of tungsten promoted zirconia (WZ) over a wide pore silica carrier (SiO_2). High dispersion of the tungsten-zirconia crystallites was achieved by a two-step controlled impregnation procedure. A first deposition of zirconia was performed by controlled hydrolysis of alkoxide. Impregnation of tungstate was performed by incipient wetness impregnation of ammonium metatungstate.

The catalysts show an activation pattern for the reaction of 1-butene similar to bulk tungsten-zirconia catalyst, with an optimum at a calcination temperature of 750 °C. Supported zirconia crystallizes almost exclusively as tetragonal crystallites.

The catalysts were tested in the reaction of hydroisomerization–cracking of *n*-octane (300 °C, 1 atm, WHSV = 1 h^{-1} and H_2/*n*-C_8 = 6 mol/mol) for the production of light isoalkanes (isobutane, isopentane, isohexane) of high octane number. The tried catalysts had a high catalytic activity and this result was related to the high surface area of the supported catalyst. Both bulk and supported catalysts deactivated rapidly if they did not contain Pt. Impregnation with Pt and the use of H_2 in the reaction medium enable the hydrogenation of coke precursors and the stabilization of the catalyst. A stable performance was obtained at a moderate activity level. This was attributed to the presence of Pt/SiO_2 particles with a stronger metal function than Pt/WZ due to a lower metal–support interaction. Silica supported catalysts would have a higher hydrogenating activity and this would be crucial for enhancing their stability in comparison to bulk Pt/WZ catalysts.

Tungsten addition to supported zirconia in amounts greater than 7.5% produced segregation of a WO_3 phase in the form of crystallites that plugged pores and produced a reduction of the available area and hence of the overall catalytic activity.

For the WZ supported catalysts activity as a function of calcination temperature had a pattern similar to that of bulk WZ catalysts. Supported WZ catalysts were more stable in the *n*-octane isomerization reaction and reached a pseudo steady state even at very low H_2 partial pressures while bulk WZ catalysts deactivated continuously and stabilized only at high H_2 partial pressures. On a mass basis of active WZ phase some supported catalysts had a higher activity than bulk WZ. They also have a more open pore structure more suitable for the reaction of bulky molecules. However the dilution effect of silica produces catalysts with a relatively low activity per unit volume.

1. Introduction

Environmental restrictions have put a stress on refiners for replacing high octane aromatics of the gasoline pool by other additives of similar high octane number and lower polluting effect. In the recent past the option of choice used to be the addition of MTBE. The latter is however being gradually banned as a gasoline additive because of recent concerns about the contamination of water reservoirs. MTBE is fairly soluble in water and contamination may arise due to spills from surface and underground storing tanks. The attention of the refiners is therefore being shifted to other sources of octane points, e.g. alkylate and branched alkanes. In the case of the latter, the usual route for obtaining C_5–C_6 branched alkanes is the isomerization of the unbranched compounds over an acidic catalyst, e.g. Pt supported over chlorided alumina or acid zeolites, as in UOP's Penex process or Shell's Hysomer processes [1]. Alternatively branched isoalkanes can also be obtained by the isomerization and cracking of long-chain

* Corresponding author. Tel.: +54 342 4571160; fax: +54 342 4531068.
E-mail address: jgrau@fiq.unl.edu.ar (J.M. Grau).

0926-860X/$ – see front matter © 2008 Elsevier B.V. All rights reserved.
doi:10.1016/j.apcata.2008.12.009

normal alkanes. While C_6–C_8 linear alkanes are usually upgraded to gasoline in the reformer to valuable aromatics and C_{10}-C_{18} linear alkanes can be sent to the kerosene and diesel pools, heavier paraffins find no use as a fuel. For example C_{20+} in vacuum gas oils are usually removed by solvent dewaxing and if not sold as paraffins they comprise an inexpensive feedstock that must be transformed again before it can be used. Another case is that of C_{18}-C_{24} and heavier waxes issuing from Fischer–Tropsch reactors. These are becoming increasingly available to refiners due to the rising price of other feedstocks and the attractiveness they have for their lack of sulfur and other impurities. All these paraffins can be advantageously adjusted in size and isomerized to branched short paraffins in one simple operation in a hydrocracking unit containing a bifunctional metal-acid catalyst [2–4].

Isomerization of heavier petroleum fractions was firstly studied as a means of lowering the pour point of jet, diesel fuels and lubricants [5]. Isomerization and selective separation of iso and normal long paraffins is indeed the basis for the process of "isodewaxing" in modern refineries [6]. In the early eighties Weitkamp [6] studied the isomerization and hydrocracking of C_6–C_{15} normal alkanes on zeolite Y loaded with Pt and Ca. Hydrocracking was not desired in this case and it was reported that at 40% conversion the amount of hydrocracking was negligible. Later similar studies on Pt/HZSM-5 zeolites [7,8], Pt/HZSM-22 zeolites [8], Pt/HY [9], Pt/HMOR [10], etc., concentrated their attention on the low boiling range C_8–C_{12} cut and hydrocracking was also assessed. When simultaneous isomerization and hydrocracking are to be considered the selectivity to gases (C_1–C_3) must be decreased.

For isomerization–cracking of long-chain *n*-alkanes a suitable catalyst which provides good isomerizing activity and a mild cracking activity should be found. Due to their good selectivity to isomers at relatively low temperatures, oxoanion promoted zirconia catalysts, like WO_3–ZrO_2 (tungsten-zirconia, WZ) or SO_4^{2-}-ZrO_2 (sulfate-zirconia, SZ) have attracted the attention of researchers. Encouraging results have been reported for isomerization–cracking of medium length model paraffins [11–15], and long (C_{16}) paraffins [14].

In the case of the SZ catalyst its most attractive feature is the high activity at low temperatures, its high selectivity to isomers and its good value of available surface area (100–200 m^2/g after activating at 550–600 °C). Certain amount of cracking is however unavoidable. The catalyst also tends to lose sulfur during operation. In the case of tungsten-zirconia, the selectivity to isomers is higher and the oxoanion is non-labile under activation or reaction conditions. However the reactor must be operated at a higher temperature and the available surface area is low (<50 m^2/g) [16,17]. The low surface is a result of the high temperature (800–850 °C) needed to pretreat the WZ catalyst. For both catalysts another concern are the mass transfer limitations arising from the big size of the long hydrocarbon chains (C_{12+}) and the relatively narrow pore diameter of SZ and WZ (10–20 Å Wheeler radius after calcination [16]).

Improved surface area and pore radii might be obtained by using special synthesis techniques to tailor the texture of zirconia but the quality of the material is usually degraded at the high temperatures needed for activity promotion. Uniform mesoporous zirconia have been successfully synthesized by means of gellation in the presence of surfactants, but the reports indicate that either the structure collapses upon calcination at relatively mild temperatures [18] or that it hasn't a higher surface than oxoanion promoted zirconia synthesized by common methods [19]. Reflux ageing of the freshly precipitated zirconia gel yields zirconia both with a uniform pore distribution and a sintering-resistant surface [20]. However oxoanion promoted catalysts based on refluxed gels have not yielded more active catalysts [17,21]. Of recent interest has been the synthesis of catalysts from zirconia aerogels [22,23]. Despite the high initial surface area both the total area and the pore volume decrease to common values after calcination.

A common way of improving the textural properties of an active catalytic phase is by dispersing it over other supports of better textural properties, like SiO_2 or Al_2O_3. Silica and alumina supported SZ catalysts have been synthesized and tested in acid-demanding reactions in the last years [12,24,25]. In the case of WZ practically no reports exist on the synthesis and use of silica supported catalysts for the reaction of alkanes.

A study of the methods of dispersion of zirconia over silica and of the use of supported Pt/tungsten-zirconia catalysts for the hydroisomerization–cracking of *n*-octane was performed in this work. Wide pore silica was chosen as carrier because of its high surface area and its wide pore network. Preparation parameters were varied and the catalysts were tested in the 1-butene isomerization, benzene hydrogenation and *n*-C_8 isomerization–cracking reactions. The catalysts were further characterized by temperature programmed techniques of desorption of pyridine, temperature programmed oxidation (TPO) of coke deposits, X-ray diffraction and sortometry. *n*-C_8 was used as model compound for isomerization–cracking as in other reports [11–14]. The test was performed both at low and high pressure. The product distribution was analyzed with a focus on the yield of branched compounds with high octane number. For this purpose the RON of the isomerizate was calculated from GC compositional data and known correlations.

2. Experimental

Due to the high complexity of the catalyst to be synthesized, a sequential approach was used: (i) synthesis of zirconia supported over silica (ZSi) of very high dispersion and resistance to sintering; (ii) promotion of ZSi with tungsten (WZSi) and activation of the thus produced catalyst; (iii) promotion of WZSi with Pt (PtWZSi) to prevent its deactivation by coking in the desired acid-catalyzed reaction.

2.1. Materials

A wide pore silica provided by Morton Thiokol (300 m^2 g^{-1}, 7 nm pore radius) was used as support. Zr *n*-propoxide was supplied by Fluka (70% in *n*-propanol). Pt hexachloroplatinate (H_2PtCl_6, 99.5%) was supplied by Aldrich. *n*-Hexane (99.9%) was supplied by Merck.

2.2. Testing of Zr impregnation method

A zirconia impregnation method had to be chosen in order to perform the synthesis of the ZSi samples. Wet impregnation with an excess of solution was compared against incipient wetness impregnation. Samples with a zirconia content of 25% Zr were prepared in both cases. These samples were named $Z^{SOL}Si$ (excess solution) and $Z^{INW}Si$ (incipient wetness). The amount of Zr deposited corresponded to the content of a catalyst with a theoretical 1 monolayer of ZrO_2, i.e., a catalyst with a layer of zirconia of 1-atom thickness and a surface atomic density of 8 Zr atoms per square nanometer. Before impregnation the silica was ground to 35–80 meshes and dried at 110 °C in a stove. Incipient wetness impregnation was performed by first dissolving Zr *n*-propoxide in *n*-hexane (1:1, v:v). This solution was used to impregnate the silica with an amount equal to its pore volume. The volume was adjusted in order to get a final 25% Zr in the final catalyst. In the case of the wet impregnation with excess solution the same amount of the (*n*-propoxide:*n*-hexane) solution to give a nominal 25% Zr in the final catalyst was used. This amount was put in a flask and further

dissolved with hexane until a ratio of 6 ml of solution per gram of silica was got. The silica was then added and the solution was gently stirred for 1 h. Finally the silica was filtered. Both the $Z^{SOL}Si$ and the $Z^{INW}Si$ samples were dried at 110 °C after impregnation in order to desorb *n*-propanol mostly formed by hydrolysis of the *n*-propoxide by the silica surface OH groups.

Due to the highly hygroscopic nature of the Zr *n*-propoxide and its tendency to react with room humidity to form hydrolysis products (e.g. $Zr(OH)_4$) the impregnation of the *n*-propoxide on the silica support was performed inside a hermetically sealed glove box and using dry nitrogen to flush the chamber between preparation steps. The solvent and the *n*-propoxide were kept closed and they were opened only inside the chamber after desiccating the atmosphere.

In order to check the degree of dispersion and interaction of the $Zr(OH)_4$ layer with the silica surface the sintering resistance was measured by first calcining $Z^{INW}Si$ and $Z^{SOL}Si$ at 600 and 800 °C in static air for 1 h in a muffle. Then the crystal size growth was assessed by means of X-ray diffraction. The size of the ZrO_2 crystallites formed was inferred from the size of the peaks of the zirconia phase.

2.3. ZSi and Zr(OH)$_4$ supports

Once the method that leads to the most dispersed and sintering-resistant ZSi catalyst was determined the preparation of the sample with 25% Zr was repeated and two additional catalysts with higher Zr content were synthesized using this method. The new Zr loadings were 33% and 39%, percentages that correspond to 1.5 and 2.0 monolayers, respectively. These supports in their fullest hydration state before calcinations were named as $ZOH^{1.0}Si$, $ZOH^{1.5}Si$ and $ZOH^{2.0}Si$. The name of these samples after calcinations was correspondingly changed to $Z^{1.0}Si$, $Z^{1.5}Si$ and $Z^{2.0}Si$.

An amorphous $Zr(OH)_4$ gel (ZOH sample) was prepared by precipitation of $ZrOCl_2{\cdot}8H_2O$ (Strem, 99.998+%) with concentrated NH_4OH (Merck, 35%). Details of the technique can be found elsewhere [26].

2.4. Tungsten promoted catalysts

Silica supported tungsten-zirconia catalysts (WZSi) were prepared by an incipient wetness technique, using the uncalcined supports, $ZOH^{1.0}Si$, $ZOH^{1.5}Si$ and $ZOH^{2.0}Si$ and an aqueous solution of ammonium metatungstate hydrate (Fluka, 99.99%). The pH of the solution was adjusted to a value of 10 in order to prevent the precipitation of tungstate species [16]. At acid and neutral pH values the formation of stable big tungstate oligomers in solution is favored by solution thermodynamics. These bulky oligomers may have great difficulties for diffusion inside the pores or they may not enter the inner pore structure at all. After impregnation of the tungsten solution the catalysts were slowly dried at 60 °C in static air. Four W loadings were used, corresponding to a W% with respect to the WZ mass of 5%, 7.5%, 10% and 15%. The final catalysts were calcined at 800 °C, in accord with previous reports that indicate that this is the optimum temperature of calcination of tungsten-zirconia catalysts and supported tungsten-zirconia [27].

Bulk tungsten-zirconia (WZ) was synthesized by incipient wetness impregnation of bulk $Zr(OH)_4$ gel (ZOH sample) with the metatungstate solution using the same procedure described above and with a W content of 15%.

2.5. Pt promoted catalysts

For the best performing catalysts Pt was added by incipient wetness impregnation from a solution of chloroplatinic acid. The impregnation volume was adjusted in order to get a Pt content of 0.5% in the final catalyst. These double promoted catalysts were named PtW^aZ^bSi. "*a*" indicates the W% on a WZ mass basis (without including the silica component; this is for comparison with bulk WZ catalysts). "*b*" indicates the zirconia contents expressed as number of theoretical monolayers.

2.6. Characterization

As explained above XRD spectra were recorded in a diffractometer (Shimadzu XD-1), using CuKα radiation filtered with Ni and scanning the $2\theta = 15–75°$ range. Crystallite size was calculated from XRD line broadening using the Scherrer equation:

$$D_v = \frac{K\lambda}{(\beta\cos\theta)}$$

where D_v = crystallite size weighted by volume, K = Scherrer constant, λ = wavelength of radiation (0.154 nm, CuKα), and β = integral breadth of peak (in radians 2θ) located at angle θ. This approach neglects the effect that strain can have on line broadening. The main peak of the tetragonal phase at $2\theta = 30°$ was used in the case of the ZrO_2 crystals and the peak at $2\theta = 23.2$ corresponding to the ⟨0 0 1⟩ reflection in the case of the WO_3 crystals.

Textural properties were measured in a Quantachrome NOVA-1000 sortometer. The specific surface area (Sg) was measured by the BET method with data of the adsorption branch of nitrogen at 77 K and the pore distribution by the BJH method with data of the desorption branch.

2.7. Temperature programmed desorption of pyridine

The quantity and amount of acid sites on the catalysts surface were assessed by means of temperature programmed desorption of pyridine. 200 mg of the catalyst were first immersed in a closed vial containing pure pyridine (Merck, 99.9%) for 4 h. Then the catalyst was taken out from the vial and excess pyridine was removed by evaporation at room temperature under a fume hood. The sample was then charged to a quartz micro reactor and a constant nitrogen flow (40 ml min^{-1}) was established. Weakly adsorbed pyridine was first desorbed in a first stage of stabilization by heating the sample at 110 °C for 2 h. The temperature of the oven was then raised to 600 °C at a heating rate of 10 °C min^{-1}. The reactor outlet was directly connected to a flame ionization detector to measure the desorption rate of pyridine.

2.8. 1-Butene reaction

Isomerization of 1-butene (Matheson, 99.5%) was performed in pulse mode in order to rapidly screen the optimum of calcination temperature with an acid-catalyzed reaction. 0.3 ml of butene were used in each pulse, the carrier was nitrogen at 10 ml min^{-1}, and the temperature of reaction was 70 °C. 0.18 g of catalyst were used in each test. The catalysts used in this acid-catalyzed reaction were calcined but not promoted with Pt because only the acid function was being evaluated and optimised.

2.9. Benzene hydrogenation

The hydrogenation of benzene to cyclohexane is a reaction that is insensitive to the structure of the metallic active site and it was used here as a test reaction of the metal function. Reaction conditions: catalyst mass = 0.15 g, 100 °C, 1 atm, benzene flow rate 0.51 ml h^{-1}, H_2/Bz = 4.6 (molar ratio). All catalysts were prereduced 1 h in H_2 at 300 °C before the reaction. Benzene was supplied

by Merck (spectroscopy grade, 99.9% pure). The specified sulfur upper limit was 0.001%.

2.10. n-Octane reaction

It was performed both at atmospheric and high pressure, using the W and Pt promoted silica supported zirconia catalysts, PtW^aZ^bSi. All conditions were similar except for the value of the pressure and the WHSV. From chromatographic data, n-C_8 conversion and yields to the different products (on a carbon basis) were calculated (for a more detailed explanation see reports [11–14]). The RON of the products mixture was calculated using the method of Walsh and Mortimer [28]. The RON gain (ΔRON) in the hydroisomerization reactor was calculated as the difference between the RON of the products mixture and the RON of n-octane (−19). *Low pressure*: 300 °C, 1 atm, WHSV = 1 h^{-1} and H_2/n-C_8 = 6 mol/mol, 1 g of catalyst per run. Before the reaction the catalysts was calcined in flowing air (10 ml min^{-1}) for 1 h at 500 °C. Then the system was flushed with nitrogen, the temperature was lowered to 300 °C and the catalyst was reduced at this temperature in hydrogen for 1 h. *High pressure*: 300 °C, 14 atm, WHSV = 4 h^{-1} and H_2/n-C_8 = 6 mol/mol, 1 g of catalyst per run.

2.11. Temperature programmed oxidation

The amount and nature of the coke deposited on the catalysts at the end of the catalytic tests were determined by means of temperature programmed oxidation. 0.04–0.06 g of the coked catalyst were loaded in a quartz reactor and stabilized in N_2. Then the nitrogen stream was replaced by a mixture of 5% O_2 in N_2 (60 ml min^{-1}) and the cell temperature was raised from 30 to 650 °C at a 10 °C min^{-1} heating rate. Coke deposits were burned and the combustion gases converted to methane and quantitatively measured in a continuous way with a flame ionization detector. The total carbon concentration of the catalyst samples was obtained by integration of the TPO trace and by reference to TPO tests of samples with a known amount of carbon.

3. Results and discussion

The synthesis of catalytically active tungsten-zirconia supported over silica poses many challenges. In order to avoid the loss of available surface area by pore plugging, agglomeration during deposition of zirconia or during crystallization of the dispersed phase must be prevented, and a high initial dispersion is desired [29]. However one of the main factors linked to the onset of the activity of tungsten-zirconia conspires against this. The activity is related to the formation of crystalline tetragonal zirconia crystallites on one side and the wetting of these crystallites by a uniform WO_x monolayer on the other [27]. In tungsten-zirconia both of these phenomena occur at very high temperatures, 700–800 °C. Pure zirconia crystallization occurs at 350 °C but crystallization is shifted to high temperatures in tungsten-zirconia due to the interference to ionic mobility posed by surface and bulk tungstate anions. Therefore in supported ZOHSi we need a high initial dispersion of the $Zr(OH)_4$ layer to avoid premature sintering before the high temperatures of activation of WZ are reached.

3.1. ZSi samples

Fig. 1 contains the XRD spectra of both $Z^{INW}Si$ and $Z^{SOL}Si$ at two high temperatures, 600 and 800 °C. It is known that roughly a crystallite with at least 10 crystal planes is necessary to produce a detectable XRD peak. It can be seen that at 600 °C crystal growth has already begun in $Z^{SOL}Si$ while in $Z^{INW}Si$ this does not occur. At 800 °C crystal growth has just began in $Z^{INW}Si$ while $Z^{SOL}Si$ is heavily sintered. These results indicate that impregnation in solution fails to produce a highly dispersed zirconia layer that in interaction with the silica surface will resist thermal sintering. For this reason incipient wetness was chosen as the impregnation method for the synthesis of the other silica supported zirconia samples.

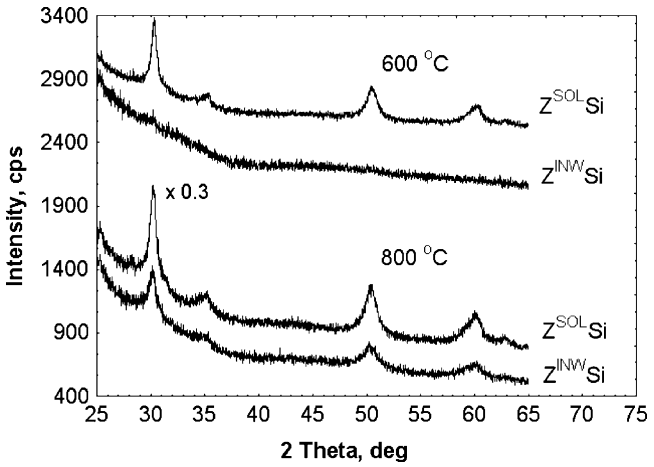

Fig. 1. XRD spectra of silica supported zirconia calcined at two different temperatures. $Z^{SOL}Si$/800 °C has been scaled down to fit into the figure.

The reason for the early crystallization of the $Z^{SOL}Si$ samples seems to be the agglomeration of $Zr(OH)_4$ particles during impregnation. Most probably the stirring of the solution during 1 h can lead to hydration from room humidity. The partial hydrolysis of n-propoxide in solution would lead to the grafting of oligomers on silica rather than the grafting of individual molecules on silanol groups. Sortometry data seem to support this. Table 1 contains data of specific surface area, pore volume and crystal phase. The $Z^{SOL}Si$ sample has a very low area even if not calcined, indicating that pore mouths that lead to the inner structure have been plugged.

In the case of the incipient wetness impregnation procedure, the fast filling of the pores prevents the hydrolysis of highly reactive Zr n-propoxide. This reaction then can only occur on surface silanols. The success of the technique is further proved by BJH pore size distributions plotted in Fig. 2. The BJH technique is fairly appropriate in the mesopore region but rather inaccurate in the micropore region. The results corresponding to the micropore region must therefore be considered on a comparative basis rather than on a rigorous quantitative one. The results indicate that there is only a gradual decrease of the total pore volume (equal to the area of the curve) when going from the silica blank to the Zr loaded

Table 1
Properties of the silica gel and the ZSi supports. A: amorphous; M: monoclinic; T: tetragonal.

Material	Vg (ml g^{-1})	Sg (m^2 g^{-1})	Phase
ZOH, 110 °C	–	157	A
Z, 800 °C	–	12	M++, T–
WZ, 800 °C	–	36	T++, M–
Si, 110 °C	–	285	A
$Z^{SOL}Si$, 110 °C	–	95	A
$Z^{SOL}Si$, 800 °C	–	78	T
$Z^{1.0}Si$, 110 °C	1.19	321	A
$Z^{1.5}Si$, 110 °C	0.95	314	A
$Z^{2.0}Si$, 110 °C	0.75	354	A
$Z^{1.0}Si$, 800 °C	–	222	T
$Z^{2.0}Si$, 800 °C	–	253	T
$W^{7.5}Z^{1.0}Si$, 800 °C	0.34	137	–
$W^{10}Z^{1.0}Si$, 800 °C	0.26	107	–
$W^{15}Z^{1.0}Si$, 800 °C	0.20	94	–

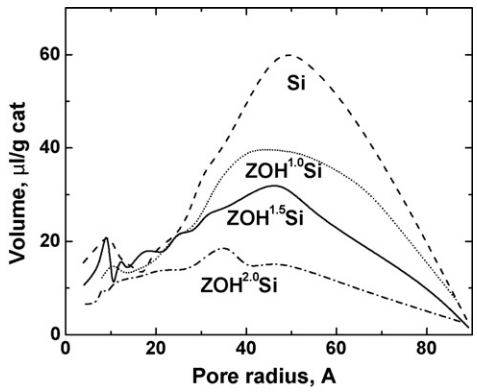

Fig. 2. BJH distribution of the silica supported zirconia samples impregnated by incipient wetness (uncalcined).

samples. As expected the center of the distributions is shifted to smaller pore radius as the Zr content is increased. In Table 1 it can also been seen that the samples impregnated by the incipient wetness procedure had even higher surface area values than the blank. This was related to the creation of some micropore structure by pillaring by Zr in small silica pores, as seen in the micropore region of the BJH plots. These structures were apparently brittle, they collapsed during calcination at high temperatures and surface area values dropped to almost 200 $m^2\,g^{-1}$ after calcination at 800 °C probably due to pore plugging by zirconia crystals.

Concerning the crystal structure the spectra of Fig. 1 clearly indicate that the crystals of silica supported zirconia are fluoritic because no peak at 28° typical of the monoclinic phase is detected. The presence of the peak at 30.5° indicates that the silica supported zirconia crystals are tetragonal. This is the phase claimed to be responsible for the onset of catalytic activity of oxoanion promoted zirconia catalysts in acid-catalyzed reactions [30]. The appearance of this phase out of its range of thermodynamic stability is due to the interaction of small crystallites with the silica surface. It has been early argued by ceramics researchers that monoclinic zirconia has a higher surface energy than tetragonal zirconia and that for this reason small crystallites are stabilized in the metastable tetragonal habitat. The interaction with the silica surface provides additional stabilization and prevents the tetragonal-to-monoclinic transition.

3.2. WZSi samples

Prevention of agglomeration and high initial dispersion are also required for the loaded tungstate species. The deposition of W from tungstate salts is complicated by the many species present in equilibrium in aqueous media and at different pH conditions. Bulky oligomeric anions of 12 W atoms ($W_{12}O_{41}{}^{10-}$) that are present in solution at neutral pH values have a diameter bigger than 2 nm and are to be prevented due to their slow diffusion and their potential plugging harm. Another factor to take into account during the impregnation is the surface charge of the support. At pH conditions in which small species are stable (pH > 9) the surface of most oxides (silica, zirconia) is negatively polarized and a coulombic repulsion exists with the anions in solution (e.g. $WO_4{}^{2-}$). However this is a less important issue when the impregnation is performed by incipient wetness because there is no way that the solute can get out of the particle pore network as it could be the case if the particles were immersed in a liquid.

After the initial dispersion of both zirconia and tungstate the main parameter controlling the texture of the final catalyst is the calcination temperature. The value of the temperature must be critically tuned due to the opposite behaviour of dispersion and onset of catalytic activity. As explained at the beginning of the discussion, oxoanion promoted zirconia catalysts which are active in acid-demanding reactions must be crystalline and tetragonal. Amorphous materials have no activity under normal conditions of preparation [31] and crystallization of zirconia involves the loss of dispersion. An optimum crystal size must be found at which activity exists and dispersion is high. This can only be done indirectly by assessing the catalytic activity.

XRD spectra of the $W^{7.5}Z^{1.0}Si$ and $W^{15}Z^{1.0}Si$ samples calcined at 500, 600, 700 and 800 °C were used to assess the crystal growth by means of Scherrer's formula for XRD peak broadening. In the case of the $W^{7.5}Z^{1.0}Si$ catalyst the zirconia particles kept almost a constant size, growing from 0.93 to 1.06 nm in the 500–800 °C calcination range. The spectra of WO_3 showed three peaks at 23.2–28.4, corresponding to reflections of the ⟨0 0 1⟩, ⟨0 2 0⟩ and ⟨1 1 1⟩ planes. No peaks due to substoichiometric oxides were found. The ⟨0 0 1⟩ peak line broadening measurements yielded the following sizes at 500, 600, 700 and 800 °C: 3.54, 2.72, 2.48 and 2.83 nm. A decrease of the WO_3 crystal size at 600–700 °C is detected. In the case of the $W^{15}Z^{1.0}Si$ catalyst the ZrO_2 particle size varied from 1.27 to 1.28 nm and the WO_3 particle size at subsequently higher temperatures was: 2.83, 1.29, 2.02, 2.82 nm. Again a reduction of the WO_3 crystallite size occurs at 600–700 °C. This can be attributed to the appearance of the phenomenon of wetting of WO_3 over ZrO_2 particles, as reported elsewhere [32]. At 800 °C the spreading of WO_3 is lower than the sintering and a net crystal size growth is seen.

3.3. 1-Butene reaction

Due to the high reactivity this reaction can easily proceed on sites of low and mild acid strength. In this sense it is sensitive to the total amount of acid sites. It was used here in order to make a rapid screening of the optimum calcination temperature. The $W^{7.5}Z^{1.0}Si$ and $W^{7.5}Z^{2.0}Si$ samples were used for this purpose. The temperature was varied between 600 and 850 °C and it was found that the maximum initial conversion of 1-butene was obtained after calcining the catalysts at 750–800 °C (see Fig. 3). The activity was practically zero at 600 °C. The samples activated at 750 °C had a higher initial activity than those activated at 800 °C but this result was reversed rapidly in the next pulses. This is surely due to deactivation by coking. As the activity of those calcined at 800 °C remained for a longer number of pulses it was considered that a greater number of acid sites were generated in this case. Calcination at 800 °C was then adopted for all samples.

3.4. Acidity assessment

Results of temperature programmed desorption of pyridine are included in Fig. 4. The results correspond to the $PtW^{7.5}Z^{b}Si$ samples

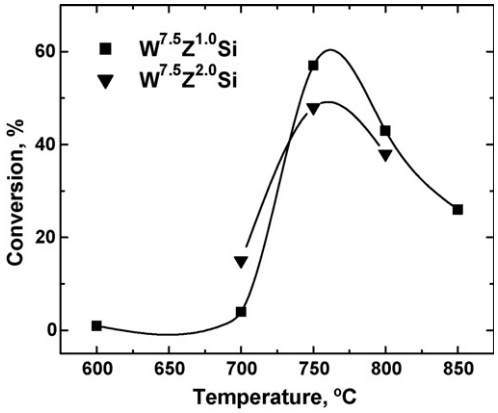

Fig. 3. Conversion of 1-butene as a function of the calcination temperature. $W^{7.5}Z^{1.0}Si$ and $W^{7.5}Z^{2.0}Si$ catalysts.

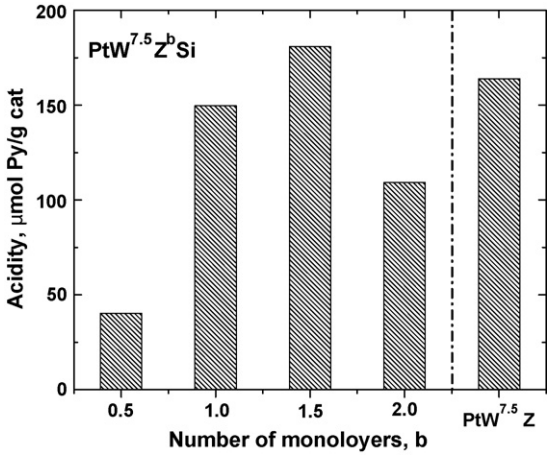

Fig. 4. Temperature programmed desorption of pyridine. Catalysts calcined at 800 °C. Influence of zirconia content.

with varying number of Zr monoloyes (b) and to the reference bulk catalyst $PtW^{7.5}Z$. It can be seen that although the amount of WZ is augmented almost four times from $W^{7.5}Z^{0.5}Si$ to $W^{7.5}Z^{2.0}Si$ the amount of acid sites generated after calcination at 800 °C is much less and not proportional. The maximum acidity generation occurs for $W^{7.5}Z^{1.5}Si$ and is similar to that of the reference bulk catalyst. The results can be explained by the size of the WZ particles. If the dispersion is not maintained from $W^{7.5}Z^{0.5}Si$ to $W^{7.5}Z^{2.0}Si$ the bigger size of WZ particles will lead to lower surface-to-volume ratios and a non-proportional increase of the acidity with Zr%. A loss of dispersion is expected due to the lower effect of interaction of the surface when the load is increased. Particularly the acidity increase is weak when increasing from 1.5 to 2.0 monolayers. In this sense in terms of acidity per unit WZ mass and taking into account the cost of the active phase, better acidity results are obtained with 1–1.5 monolayers.

Total acidity in catalysts for isomerization–cracking has been found to be the most important parameter controlling the total activity because the reaction does not require very strong acid sites and almost all sites can participate of the reaction [4,33].

3.5. Benzene reaction

Hydrogenation of benzene to cyclohexane is a structure-insensitive reaction and is a useful test for assessing the hydrogenating activity of the metal function. All catalysts tested had the same Pt content. Cyclohexane was the only one product formed. The results revealed similarities among all supported catalysts but great differences with the bulk PtWZ catalyst. The values of conversion of benzene to cyclohexane on $PtW^{7.5}Z^{b}Si$ were 36%, 33% and 29% for b = 0.5, 1.0 and 1.5 monolayers, respectively. In the case of the bulk $PtW^{7.5}Z$ catalyst the benzene conversion was only 7%. It can be seen that the conversion values for the supported catalysts were much greater than those for the bulk catalysts. The results can be explained by considering that there exists a different interaction between the Pt particles and the support in the case of the bulk and silica supported catalysts. In PtWZSi catalysts some Pt particles can be supported on the silica surface and away from WZ particles. For these particles the only metal–support interaction is that between Pt and silica, largely documented to be mild and with no severe effects on the metal properties of Pt. In the case of the bulk PtWZ catalysts there is no way the Pt particles can avoid the harmful Pt–WZ metal–support interaction. This interaction is less strong than that found in Pt/sulfated-zirconia catalysts but it is strong enough to decrease H_2 chemisorption to negligible values [13,34].

A similar effect of enhancement of Pt metal properties by supporting its particles on silica has been previously reported in the case of the sulfate-zirconia (SZ) catalysts. Grau et al. [12] supported SO_4^{2-}-ZrO_2 over silica and used controlled pH conditions to deposit Pt selectively over the silica support. The thus prepared catalysts showed enhanced stability in the hydroisomerization–cracking of long paraffins as compared to bulk catalysts. In our case if we compare the results of metal activity of the PtWZ catalyst and the silica supported ones with 1 or 1.5 monolayers, it can be seen that in spite of having a similar total acidity (see Fig. 4) their metal activity differs greatly. This is likely due to the contribution of the Pt/SiO_2 particles. These particles would be crucial for activating hydrogen that spills over the catalyst surface to hydrogenate coke precursors thus keeping acid sites clean and maintaining a stable acid activity.

3.6. n-Octane reaction

The results of isomerization–cracking of n-octane at atmospheric pressure are included in Fig. 5 and Table 2. All supported WZ samples tested showed an improved stability with respect to bulk WZ, they had high values of conversion and a good selectivity to isomers. The stability was good despite the adverse process conditions (low hydrogen partial pressure). The results of Fig. 5 also indicate that the silica supported catalysts have a lower conversion drop between 5 and 210 min and that they achieve a pseudo steady state at 100 min. Such state is not achieved by the reference bulk catalysts. These have a higher conversion drop and continue to deactivate even at the end of the run. The conversion values at 3.5 h of time-on-stream and by unit mass of WZ are higher for the supported catalysts used. It must be recalled that the WZ content of the supported WZSi catalysts was 30–40%.

At 5 min time-on-stream the bulk reference catalysts had a conversion of 94.8% (catalyst with 7.5% W) and 85% (catalyst with 5% W). The silica supported catalysts with 1 monolayer of zirconia had the maximum activity (77–81%). 1.5 monolayer catalysts display an initial conversion of 46–52%. 0.5 monolayer catalysts have a conversion of 22–24% and 2 monolayer catalysts had a conversion lower than 15% (not included in Fig. 5).

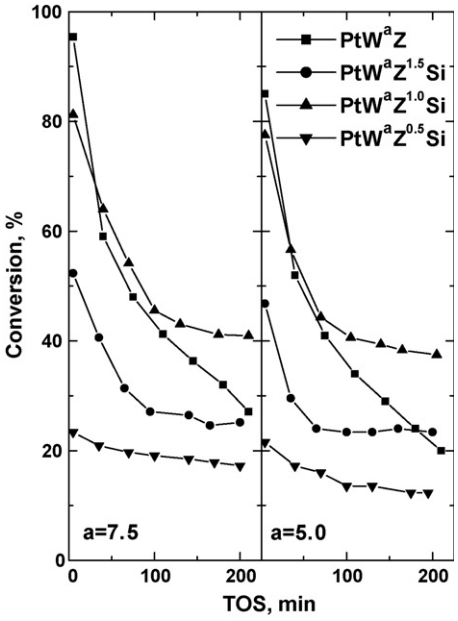

Fig. 5. Conversion of n-octane at atmospheric pressure as a function of time-on-stream. Bulk (PtW^aZ) and supported (PtW^aZ^bSi) catalysts. a = W content (% relative to WZ mass); b = ZrO_2 content (monolayers).

Table 2
n-Octane reaction (1 atm total pressure). Yield (Y_i) to different products at 3.5 h time-on-stream. C_3: propane; *n*-C_4: *n*-butane; *n*-C_5: *n*-pentane; *i*C_4: isobutene; iC_5: isopentane; iC_6: isohexanes; iC_7: isoheptanes; iC_8-MB: monobranched isooctanes; iC_8-DB: dibranched isooctanes; iC_8-TB: tribranched isooctanes.

	PtW^{a}Z	PtW^{a}Z^{b}Si			PtW^{a}Z	PtW^{a}Z^{b}Si		
a	7.5	7.5			5.0	5.0		
b	–	0.5	1.0	1.5	–	0.5	1.0	1.5
Y_{C_3}	0.2	0.7	2.2	1.5	0.1	0.8	1.7	1.2
Y_{n-C_4}	0.2	1.8	3.3	3.1	0.1	2.1	3.9	2.7
Y_{n-C_5}	0.1	0.4	0.9	0.9	0.1	0.4	0.6	0.8
Y_{iC_4}	0.4	3.5	7.5	5.8	0.3	3.5	7.4	4.7
Y_{iC_5}	0.1	0.7	2.5	2.0	0.2	0.8	1.9	1.2
$Y_{iC_6-iC_7}$	0.1	0.6	0.2	0.5	0.1	0.7	0.2	0.5
Y_{iC_8-MR}	19.0	6.6	16.4	7.6	15.1	3.6	14.6	8.2
Y_{iC_8-DR}	5.5	1.9	5.5	2.1	4.1	0.8	4.7	2.3
Y_{iC_8-TR}	0.8	0.5	1.7	1.2	0.5	0.2	1.6	1.1

a = W content (% relative to WZ mass). *b* = ZrO_2 content (monolayers).

At 3.5 h time-on-stream the 1 monolayer ZrO_2 catalysts had a higher conversion than bulk WZ ($W^{5.0}Z$ = 20.1%, $W^{7.5}Z$ = 27.3%, W^5Z^1Si = 37.4%, $W^{7.5}Z^1Si$ = 40.9%). This difference is more marked when considering the activity per unit of WZ mass ($W^{5.0}Z$ = 20.1%, $W^{7.5}Z$ = 27.3%, W^5Z^1Si = 120.2%, $W^{7.5}Z^1Si$ = 124.3%). $PtW^{7.5}Z^{1.0}Si$ and $PtW^{5.0}Z^{1.0}Si$ were the most active and stable of all the catalysts tested.

With respect to the selectivity Table 2 shows the distribution of products obtained with the reference catalysts and with the silica supported catalysts. The results are expressed in terms of values of yield to the different products at 3.5 h of time-on-stream. The bulk catalysts display a great loss of the cracking activity with time-on-stream. At the end of the run their selectivity is biased completely to the formation of C_8 isoparaffins. The formation of light gases and cracking products becomes negligible (<1.1%). A closer look at the isomers distribution reveals that C_8 isoparaffins formed on bulk PtWZ catalysts are mostly monobranched methyl heptanes. This is also a sign of a decreased acid activity. Multiple branching becomes precluded due to a low acid site density or to the coking of the stronger acid sites. In contrast the silica supported PtWZ catalysts keep a meaningful residual cracking activity after reaching their activity pseudo steady state. This cracking activity is mainly directed towards forming isobutane. The persistence of the cracking activity is an indicator of the active role of the metal function in keeping strong acid sites free of coke and with ability to cleave C–C bonds. The metal function must activate hydrogen that migrates to these sites to hydrogenate oligomeric precursors of coke. The isomers distribution on PtWZSi catalysts at the end of the run is enriched in di and tribranched isooctanes.

In order to verify the higher stability of the silica supported catalysts the coke content on the catalysts was measured by means of TPO. Fig. 6 shows the results obtained with the 7.5% W catalysts series. It can be seen that the TPO trace of the bulk PtWZ catalyst has the biggest area (%C = 1.61) and has one single maximum at about 475 °C indicating that all carbon deposits are located on hydrogen deficient acid sites. In contrast the three silica supported catalysts have TPO traces of lower total area and their maxima are shifted to lower temperatures, (415–427 °C) indicating that coke deposits are more hydrogenated than those on bulk PtWZ. The carbon content values on the supported samples were 0.67%, 0.49% and 0.23% for the catalysts with 1.5, 1.0 and 0.5 monolayers, respectively.

If we see the data of Fig. 5 corresponding to the initial (5 min) and final (210 min) activity at low pressure (1 atm) we can see that for a fixed amount of zirconia (number of monolayers) the activity is fairly insensitive to the content of tungsten though in Table 2 it can be seen that the selectivity to isooctanes is a little higher. This could be related to a phenomenon of segregation of bulk WO_3 at high tungsten loadings. If a small amount of W becomes grafted on zirconia after calcining at 800 °C and the rest segregates and sinters to form isolated WO_3 crystals most of the activity is likely to be related to a small fraction of the deposited tungsten.

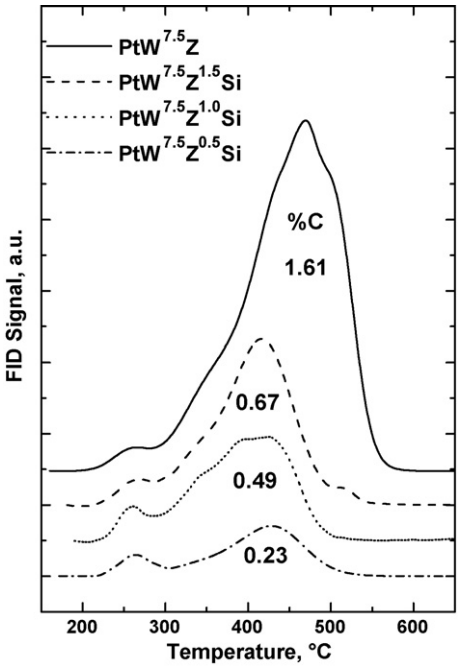

Fig. 6. TPO of the carbon deposits formed on the catalysts after the *n*-octane reaction (1 atm, 3.5 h time-on-stream). $PtW^{7.5}Z$ (bulk) and $PtW^{7.5}Z^bSi$ (supported) catalysts. *b* = 0.5, 1.0, 1.5 monolayers.

In order to check the previous hypotheses one catalyst series was chosen with regards to its activity in hydroisomerization of *n*-octane at low pressure and it was further tested at higher pressures. Supported zirconia catalysts with 1 monolayer zirconia content and 7.5%, 10% and 15% W were thus used and the results can be seen in Fig. 7. There is a clear trend of decreasing activity at increasing W contents. For the 7.5% W catalyst the conversion is 96.7% while for the 15% W catalyst the conversion drops to 39.7%. The 10% W catalyst shows an intermediate value of 80.3%. It can also be seen that the selectivity to iC_8 isomers and the ΔRON are decreased at higher W contents. It turns out that the $PtW^{7.5}Z^{1.0}Si$ catalyst has optimal catalytic properties of conversion, selectivity (20.4% isooctanes and 73.9% to total isoparaffins) and RON gain (96.1%) and is a very promising material for the hydrocracking of long alkanes.

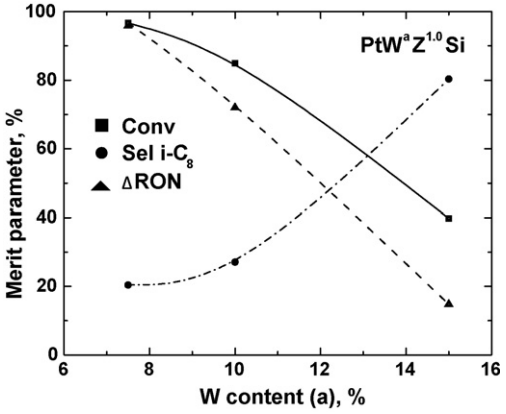

Fig. 7. *n*-Octane reaction at 14 atm. Merit parameter (conversion, octane gain, selectivity to isooctanes) values at 3 h time-on-stream, as a function of W content (% relative to WZ mass, *a*).

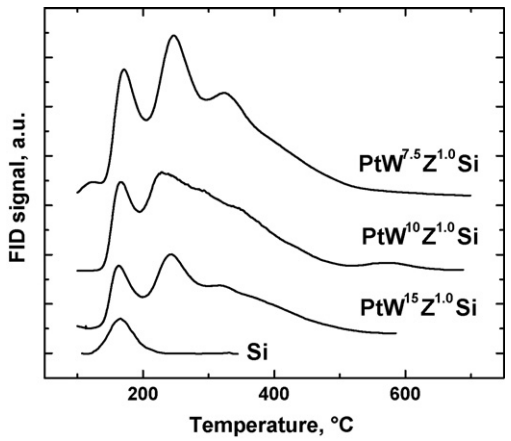

Fig. 8. Temperature programmed desorption of pyridine. Influence of tungsten content (*a*). PtW^{a}Z$^{1.0}$Si catalysts.

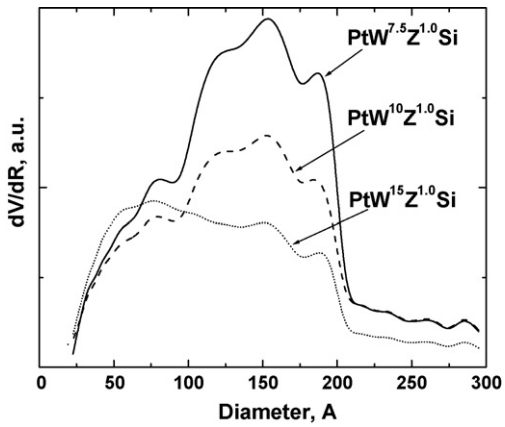

Fig. 9. Pore size distribution (d*V*/d*R*). Influence of tungsten content (*a*). PtW^{a}Z$^{1.0}$Si catalysts.

An insight into the reasons for the influence of W on the activity pattern can be got when inspecting both textural and acidity results of the supported WZ catalysts. The results of Table 1 indicate that both the specific surface area and the pore volume greatly decrease as the W content is increased. This is attributed to the sintering of the supported W element into WO_3 crystals that plug some portions of the pore structure. Crystal growth of WO_3 upon calcination was detected in two ways. By visual inspection the W containing catalyst developed a light green colour after calcinations and the intensity of the colour increased with the W content. XRD spectra of these catalysts further revealed that indeed WO_3 crystals were formed. Three peaks between $2\theta = 22–25^\circ$ could be clearly identified in the WZ supported catalysts and were identical to those found in the spectrum recorded for a WO_3 blank. The peaks appeared after calcination at 800 °C but were completely absent in the spectra of samples calcined at 600 °C.

The pyridine TPD traces of three supported WZ catalysts (1 monolayer ZrO_2, 7.5%, 10% and 15% W) and that of the blank are included in Fig. 8. All the silica supported zirconia TPD traces have the same shape and a similar proportion of trace area in the low temperature region (100–250 °C) and the high temperature one (250–500 °C). This indicates that the ratio of the concentration of sites of acid strength high/(low + mild) is the same for all the catalysts tested. The total TPD trace area decreases as the W content is increased. The invariance of the TPD trace pattern and the decreasing area as a function of the W content seem to indicate a mechanism of pore plugging already posed in the previous paragraphs. Only a small amount of W becomes dispersed over the ZrO_2 particles during the calcination treatment and the rest is sintered into isolated WO_3 crystals. The crystals WO_3 coalesce and grow until they reach the size of some pores and block the passage of reactives and reactants to some inner areas of the catalysts. The volume of the WO_3 segregated phase greatly grows in the 10% and 15% W samples indicating that the most suitable W content is 7.5%.

A confirmation of a segregation phenomenon taking place is obtained by inspecting the pore size distribution plots of the W doped catalysts (Fig. 9). It can be clearly seen that W doping severely reduces the mesopore volume while keeping the micropore volume intact. The invariance of the micropore volume must be related to a problem of diffusion of metatungstate anions inside the micropores during impregnation. In this way most WO_3 is formed solely in the mesopores when crystallization and sintering of this phase occurs. The decrease of the total pore volume must be associated to a parallel decrease of the available surface area. This volume decrease must be both to the occupancy of part of this volume by WO_3 and by the blocking of some pores that inhibits the access to the inner pore structure.

The formation of WO_3 crystals was detected both by XRD and by visual inspection. It is known that WO_x species do not absorb in the visible region of the light spectrum while bulk WO_3 have a green colour. Colour was indeed developed in W doped samples after calcining at 800 °C and the intensity grew at higher W dopings. The formation of this segregated phase must be addressed mainly to a mismatch between the thermally activated sintering of the zirconia phase and the W promoter. Zirconia starts to sinter at 550–600 °C while the phenomena of W mobility and W spreading due to differences in surface tension appear at higher temperatures. If zirconia crystallites are first formed their physical separation from W makes it difficult for W species to migrate and be stabilized over zirconia. The small silica–tungsten interaction and this physical separation conspire to promote the nucleation of segregated WO_3 crystals.

A comparison of the performance of zeolitic catalysts and WZSi catalysts in hydroisomerization–cracking of long paraffins is included in Table 3. The comparison is done against the best values obtained with one supported WZ catalyst. Commercial catalysts tested under similar temperature conditions were chosen. All the results of the commercial catalysts were obtained at higher residence time values (W/F). In spite of the less favorable conditions, the comparison shows that the second highest conversion (96.7%) and the highest yield of total branched isomers (iC_4–iC_8 = 71.5%) are obtained with the supported WZ catalyst. The

Table 3
Comparison of current and previously reported results on the isomerization–cracking of long-chain alkanes. Results at 3 h time-on-stream.

Catalysts	Feed	T (°C)	P_{HC} (psi)	W/F_{HC} (g h mol^{-1})	Conversion (%)	S_{iso} (%)[b]	Yield$_{iso}$ (%)[c]	Ref.
Pt(0.5%)/CaY	*n*-C_9	275	32	138	76.4	87.8	67.1	[1]
Pt(0.3%)/H-MOR	*n*-C_8	300	29.4	60	67.9	24.2	16.4	[10]
Pt(0.5%)/HZSM-5	*n*-C_9	280	2.8	130	98.5	18.9	18.6	[6]
Pt(0.5%)W$^{7.5}$Z$^{1.0}$Si	*n*-C_8	300	14	28	96.7	73.9	71.5	[a]

[a] This work.
[b] $S_{iso} = \Sigma X_i$ (conversion, compound i)/X_T (total conversion) × 100. i: isomers.
[c] Yield$_{iso} = \Sigma X_i$ (conversion, compound i) × 100. i: isomers.

zeolitic catalyst with the highest conversion was the Pt/H-ZSM5 one. Though it had 98% conversion most products were light compounds produced by cracking and therefore the yield to branched isomers was very low, 17%.

Another important comparison that should be made is that between bulk tungsten-zirconia (WZ) and supported tungsten-zirconia (WZSi). If we focus on the activity per unit mass of WZ, dispersion over silica can in some cases produce a higher intrinsic activity of the active phase. This is good from the point of view of the final cost of the catalyst because the price of the silica support is supposed to be much smaller than the price of tungsten-zirconia. From the point of view of the catalytic activity per unit reactor volume the conclusion is different. Due to the low density of silica, dispersion of the WZ active phase produces a great dilution effect and as a consequence the activity of bulk WZ is superior. This is important in those cases where a very active WZ catalyst per unit volume is needed for the revamping of some process units.

4. Conclusions

Supported ZrO_2 of high dispersion can be synthesized by incipient wetness impregnation of Zr alkoxide. The resistance to sintering of this support is very good and enables the preparation of supported tungsten-zirconia which can be activated at 750–800 °C producing active sites for acid-catalyzed reactions in a similar way as standard tungsten-zirconia catalysts.

Zirconia contents next to the monolayer value (1.0–1.5 monolayers) yield the most active catalysts. The activity of supported WZ per unit mass of WZ is in most cases higher than the activity of bulk WZ and it has a good selectivity to isomers but on a volume basis the dilution effect of silica cannot be counter-balanced. Therefore it is suggested that supported WZ can replace bulk WZ in some applications where high catalytic activity per unit volume is not required.

The new catalysts are promising but the amount and conditions of impregnation of W must be revised because high W contents lead to the formation of crystals of WO_3 during calcination at 800 °C and this is an inactive phase for reactions that require medium and high acid strength.

The silica supported tungsten-zirconia catalyst that performs best in the *n*-octane test reaction is the $PtW^{7.5}Z^{1.0}Si$ one. It has optimum activity, isooctane selectivity and RON gain and thus is an optimum material for the transformation of heavy paraffinic feedstocks into high RON compounds for the gasoline pool.

Silica supported tungsten-zirconia catalysts allow similar or higher conversion levels for the same amount of active WZ phase. They are more stable and show a robust conversion of long paraffins to multibranched isomers.

Acknowledgements

We are indebted to CONICET (PIP 5423) and Universidad Nacional del Litoral for financially supporting this work. M.E. Lovato is grateful for the support she received during her stay at INCAPE labs.

References

[1] J. Weitkamp, Ind. Eng. Chem. Prod. Res. Dev. 21 (1982) 550.
[2] J.M. Grau, C.R. Vera, J.M. Parera, Appl. Catal. A 227 (2002) 217.
[3] J.M. Yori, J.M. Grau, V.M. Benitez, C.R. Vera, C.L. Pieck, J.M. Parera, Catal. Lett. 100 (2005) 67.
[4] V.M. Benitez, J.C. Yori, J.M. Grau, C.L. Pieck, C.R. Vera, Energy Fuels 20 (2006) 422.
[5] A. Chica, A. Corma, J. Catal. 187 (1999) 167.
[6] J. Weitkamp, P.A. Jacobs, J.A. Martens, Appl. Catal. 8 (1983) 123.
[7] J.A. Martens, R. Parton, L. Uytterhoeven, P.A. Jacobs, G.F. Froment, Appl. Catal. 76 (1991) 95.
[8] M. Steijns, G.F. Froment, P.A. Jacobs, J.B. Uytterhoeven, J. Weitkamp, Ind. Eng. Chem. Prod. Res. Dev. 20 (1981) 654.
[9] F. Alvarez, F.R. Ribeiro, G. Perot, C. Thomazeau, M. Guisnet, J. Catal. 162 (1996) 179.
[10] J.M. Grau, J.M. Parera, Appl. Catal. A 106 (1993) 27.
[11] J.M. Grau, J.M. Parera, Appl. Catal. A 162 (1997) 17.
[12] J.M. Grau, C.R. Vera, J.M. Parera, Appl. Catal. A 172 (1998) 311.
[13] J.M. Grau, J.C. Yori, J.M. Parera, Appl. Catal. A 213 (2001) 247.
[14] S. Zhang, Y. Zhang, J.W. Tierney, I. Wender, Appl. Catal. A 193 (2000) 155.
[15] J.C. Yori, R.J. Gastaldo, V.M. Benitez, C.L. Pieck, C.R. Vera, J.M. Grau, Catal. Today 133–135 (2008) 339.
[16] J.C. Yori, C.R. Vera, J.M. Parera, Appl. Catal. A 163 (1997) 165.
[17] J.G. Santiesteban, J.C. Vartuli, S. Han, R.D. Bastian, R.D. Chang, J. Catal. 168 (1997) 431.
[18] J.S. Reddy, A. Sayari, Catal. Lett. 38 (1996) 219.
[19] D.J. McIntosh, R.A. Kydd, Microporous Mesoporous Mater. 37 (2000) 281.
[20] G.K. Chuah, S. Jaenicke, S.A. Cheong, K.S. Chan, Appl. Catal. A 145 (1996) 267.
[21] C.R. Vera, K. Shimizu, in: Proceedings of the 82th Japan Catalysis Conference, Matsuyama, Japan, September, (1998), p. 272.
[22] D.A. Ward, E.I. Ko, J. Catal. 150 (1994) 18.
[23] R.A. Boyse, E.I. Ko, J. Catal. 171 (1997) 191.
[24] C.R. Vera, C.L. Pieck, K. Shimizu, J.M. Parera, Stud. Surf. Sci. Catal. 118 (1998) 369.
[25] T. Lei, J.S. Xu, Y. Tang, W.M. Hua, Z. Gao, Appl. Catal. A 192 (2000) 181.
[26] M. Hino, K. Arata, J. Chem. Soc. Chem. Commun. (1987) 1259.
[27] K. Arata, M. Hino, in: Proceedings of the 9th International Congress on Catalysis (Oxide Catalysts and Catalyst Development), The Chemical Institute of Canada, Ontario, 1988, p. 1727.
[28] R.P. Walsh, J.V. Mortimer, Hydrocarbon Process. 50 (1971) 153–158.
[29] S. Damyanova, P. Grange, B. Delmon, J. Catal. 168 (1997) 421.
[30] J.M. Grau, J.C. Yori, C.R. Vera, F.C. Lovey, A.M. Condó, J.M. Parera, Appl. Catal. A 265 (2004) 141.
[31] R.A. Comelli, C.R. Vera, J.M. Parera, J. Catal. 151 (1995) 96.
[32] J. Leyrer, R. Margraf, E. Taglauer, H. Knőzinger, Surf. Sci. 201 (1988) 603.
[33] J.M. Grau, V.M. Benitez, J.C. Yori, C.R. Vera, J.F. Padilhas, L.A. Magalhaes Pontes, A.O.S. Silva, Energy Fuels 21 (2007) 1390.
[34] J.G. Santiesteban, D.C. Calabro, W.S. Borghard, C.D. Chang, J.C. Vartuli, Y.P. Tsao, M.A. Natal-Santiago, R.D. Bastian, J. Catal. 183 (2) (1999) 314.